

# Multi-Variate Visualization of Cardiac Virtual Tissue

J W Handley  
K W Brodlie  
School of Computing  
University of Leeds  
Leeds LS2 9JT  
United Kingdom  
jwh@comp.leeds.ac.uk  
kwb@comp.leeds.ac.uk

R H Clayton  
University of Sheffield  
Department of Computer Science  
Regent Court  
211 Portobello Street  
Sheffield S1 4DP  
United Kingdom  
r.clayton@dcs.shef.ac.uk

## Abstract

*In standard analysis of cardiac models, typically one variable – usually the trans-membrane potential – is used in the generation of visualizations. However, all but the most basic models have many state variables at each node, information that is not used when visualizing the output of the model. In this paper, we present a novel approach to visualizing the entire state of a 2D cardiac virtual tissue.*

## 1 Introduction

Cardiac arrhythmias associated with heart disease are an important cause of premature death in the industrialised world, but the mechanisms that initiate and sustain the lethal arrhythmias of ventricular fibrillation (VF) and ventricular tachycardia (VT) remain poorly understood. Experimental and clinical studies of VF mechanisms are limited because it is difficult to record electrical activity throughout the 3D ventricular wall, and most studies are limited to surface recordings. Computational models of action potential propagation in cardiac tissue (cardiac virtual tissues - CVT) have been used extensively in the last decade to probe the mechanisms of VF [1]. The current generation of high performance computers enable simulations of VF in anatomically detailed geometries [2, 3], and many recent publications combine experimental and modelling studies [4]. In these detailed simula-

tions, the results are typically visualized using standard techniques based on a single model parameter – the trans-membrane voltage, or action potential – leading to images such as those shown in Figure 1 (see [5] for another example.) The action potential propagation is, in many ways, the heartbeat — and so it is the most important state variable of the heart model to visualize. However, it is expected that being able to visualize some or all of the other state variables may provide insight into why the normal action potential propagation breaks down into the circulating pattern of re-entry.

In cardiac tissue, propagation of the action potential depends on the state variables that determine the conductance of ion channels in the cell membrane. Visualizing these parameters as well as the action potential itself may give greater insight into normal and abnormal patterns of propagation than conventional approaches. In this paper we use simulations of 2D CVT as a first step to developing more sophisticated visualization techniques that enable one to examine the *entire* state of the simulation, not just a single variable.

## 2 Visualizing Cardiac Virtual Tissue

In the CVTs used throughout this paper, action potential propagation is modelled by a reaction diffusion partial differential equation [6], where the diffusion term describes the spread of membrane voltage from one cell to its neighbours, and the reaction term describes dynamic behaviour of the voltage difference across the cell membrane. Several different excitation

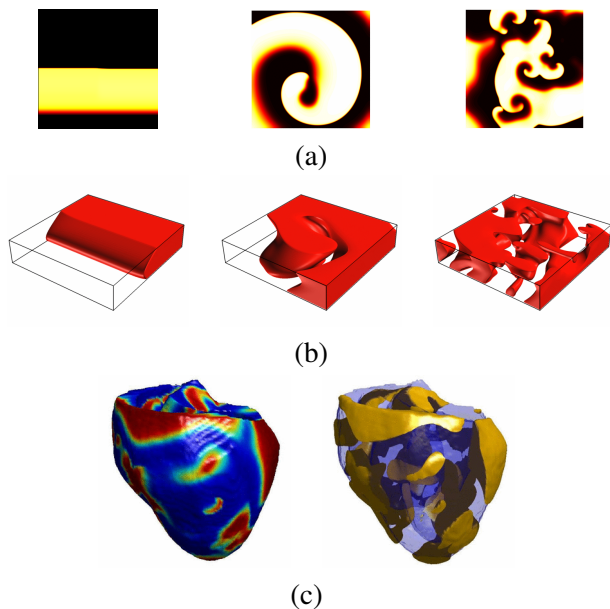


**Figure 1. Example visualizations of 2D and 3D cardiac virtual tissues. (a) 2D tissue with normal propagation (left) and re-entrant propagation with one (middle) and many (right) re-entrant waves visualized using a colourmap. (b) 3D slab geometry, with wavefronts visualized as isosurface. (c) Colourmap of membrane potential on the heart surface (left) and isosurfaces (right).**

models can be used to describe the reaction term, and these range from simplified models with 3 or 4 state variables, to more detailed models with tens of state variables [7]. The equations are solved across a grid, and typical grid geometries are a 2D sheet, a 3D slab, or an anatomically detailed representation of the heart ventricles.

The visualization challenge can be grasped very quickly through looking at the outputs of two different 2D cardiac virtual tissues. Figure 2 shows a snapshot of the state of a 2D CVT in which a re-entrant wave is rotating. In this model excitability is simulated with the simplified 4 variable Fenton Karma model [8] and in this visualization each state variable is visualized separately. Figure 3 shows a similar snapshot of a propagating plane wave in a CVT where excitability is modelled using a modification of the biophys-

ically detailed Luo-Rudy 2 model [9], which has 14 state variables. It is much more difficult to assimilate the 14 images of Figure 3 into a single mental model of the state of the simulation than the four images of Figure 2.

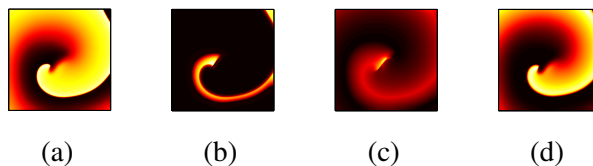


**Figure 2. A snapshot of re-entry in a 2D model with excitation described by the 4 variable Fenton Karma model [8]. The four state variables (a) U, (b) V, (c) W, and (d) D are shown individually using the hot colourmap where low brightness corresponds to low values.**

The problem of trying to assimilate a number of data sources is well known; up to 50% of humans apparently cannot fully assimilate even *one* video stream due to inattentive blindness [10]. Related to this is change blindness [11], where a significant change in a scene (for example, a tall man being replaced by a short woman) may go undetected if attention is focused elsewhere at the time of the change. We also know that attempting to perform more than one focal task at once leads to performance degradation in those tasks, as observed in driving [12] and avionics [13].

The multi-variate multi-dimensional data of CVT must therefore be converted down to a (visually) simpler representation if the entire state of the model is to be visualized. CVT data exist in two or three spatial dimensions and one temporal dimension, and these dimensions must be preserved in the resulting visualization. This means the high-variate space must be converted to an (ideally) uni-variate space. The resulting uni-variate four-dimensional data would then be straightforward to visualize using, for example, animations of iso-surfaces or volume rendering.

There are, of course, many existing techniques for visualizing multi-variate data, such as parallel coordinates, iconic representations or ‘glyphs’, and a review of these and other approaches to the visualization of complex data can be found in [14]. None of these

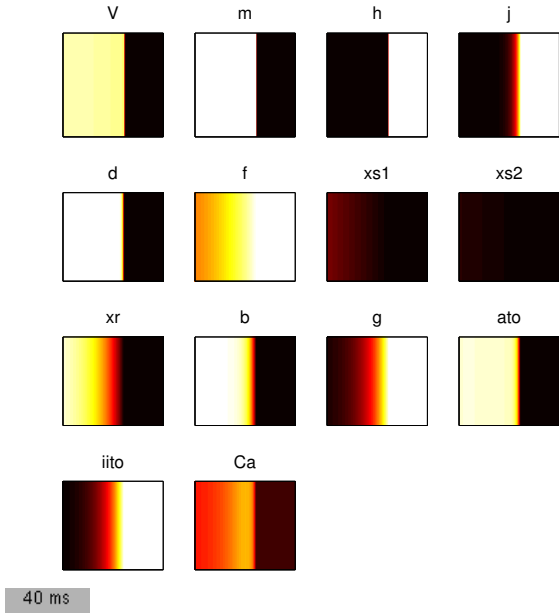


**Figure 3. Snapshot of a propagating plane wave in a 2D model with excitation described by the biophysically detailed Luo-Rudy 2 model [9]. As with Figure 2, each state variable is shown individually, except in this model there are 14 state variables.**

techniques, however, successfully handle data that are (and need to remain) four dimensional while also being (highly) multi-variate.

### 3 Visualizing in Phase Space

The nature of the propagation of action potential through the heart imposes a structure of sorts, and this structure becomes apparent, at least with more simple models, when the data is visualized in *phase space*. In the case of a tri-variate model, if the standard visualization at time  $t$  is to generate three  $n$  by  $m$  pixel images  $U_t(x, y)$ ,  $V_t(x, y)$ , and  $W_t(x, y)$ , for  $0 < x < n$  and  $0 < y < m$ , the phase space visualization is a single 3D scatter-plot obtained by plotting  $n \times m$  ‘dots’, one at each  $(U_t(x, y), V_t(x, y), W_t(x, y))$ . Figure 4 shows examples of phase space plots from a Fenton-Karma 3 variable model.

In Figure 4 the inherent structure is clearly visible

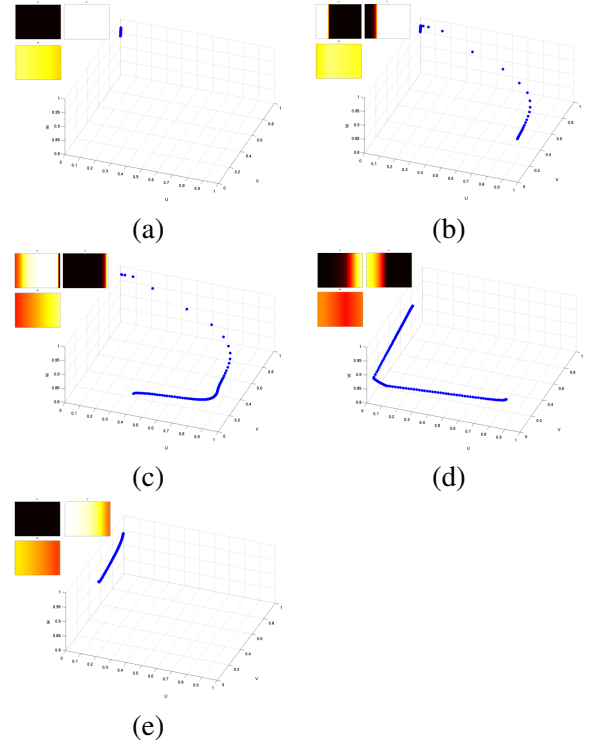


**Figure 4. A phase space plot of the 3 parameters from a 2D Fenton-Karma 3 variable model, showing the normal propagation of a wave of action potential at various intervals. The insets show the false colour images of the three variables. (a) rest state – the points occupy  $[U = 0, V = 1, W = 1]$ , (b) 30 ms after wave initiation along the left edge of the medium, (c) 90 ms, (d) 150 ms, (e) 210 ms.**

as a ‘snake’ traversing a circuit in phase space. While this ‘snake’ is entirely expected – it occurs as cells depolarise then recover – it nevertheless provides an interesting view on wavefront propagation, *and should be present even in higher variate models*.

Even more interesting effects can be observed if re-entry is induced in the model. This was achieved by changing the cell types of a circular region of tissue in the centre of the model, so that these cells take longer to recover after excitation. In this heterogeneous CVT, the normal propagation breaks down into re-entry under repeated stimulation of the tissue. As Figure 5(b) and (c) shows, the points that previously followed a

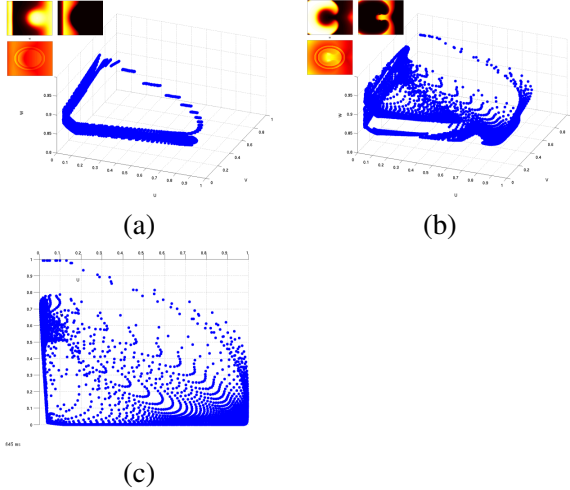


**Figure 5. A phase space plot of the 3 parameters from a 2D Fenton-Karma 3 variable model, showing re-entrant behaviour. (a) The initiation of the second stimulus — the stimulus that causes re-entry. (b) 145 ms later, when re-entry is well established. (c) A plan view of (b).**

nominal circumference have now collapsed to almost entirely fill the enclosed space.

Even this simple phase space ‘snake’ provides a novel view of the structure of the model, particularly when re-entrant behaviour is starting or stopping, and it is expected to be useful even with higher-variate models through judicious choice of the subset of variables plotted. It should be noted that adjacent points in real space can be joined in phase space, but we found this cluttered the images without providing any further insight — an intuitive ‘join-the-dots’ interpretation being the correct one.

#### 4 Visualizing many Variables

Clearly the phase space is trivial to visualize with two or three variables, but in the case of the Luo-Rudy-2 model, with 14 variables, this approach is non-trivial. One approach is to create multiple phase space plots, which has the advantage that all the data are shown, but the disadvantages of still having to focus and visually combine many data sources. The phase space

plots also have the disadvantage of removing spatial information from the visualization. Both these disadvantages can be addressed by performing some form of clustering in phase space, and using the resulting clusters to colour a spatial image.

As a starting point, we used a very simple partitioning of the  $n$ -dimensional phase space as the clustering metric, in an analogous fashion to a histogram. The 3D phase space from the Fenton Karma 3 variable model was partitioned into 1000 cuboids of equal volume, with 10 along each axis.

Once partitioned, each point in phase space falls into exactly one cuboid, and the number of points within each cuboid can be counted as if it was a histogram. However, we know the  $(x, y)$  cell that gave rise to any given point in phase space, and so we can now give each  $(x, y)$  cell a ‘hyper-histogram’ count, and use this number to generate a false colour image. Figure 6 pictorially represents the steps involved in process, with the only refinement being that only those cuboids containing more than 22 points are shown. In terms of interpreting the images formed, two cells of similar colour occupy a similarly dense region of phase space, although the regions may be quite distinct in phase space.

An alternative metric is to assign each cuboid an arbitrary ID number, and these IDs be used to generate an image. In the images thus formed, two cells of the same colour occupy the same region of phase-space, and two cells of similar colour should occupy a similar region in phase-space. Depending on the assignment of identification, the colour may also indicate the absolute or relative region of phase space given cells occupy.

Figures 7 and 8 show examples of images formed in this way, corresponding to the data presented in Figures 4 and 5. In Figure 7, the hyper-histogram counts were used to colour the images. In Figure 8, the hyper-histogram numbering method was used, with the cuboid labels ranging from 0 to 1000, strictly increasing along the  $U$ ,  $V$ , and  $W$  axis, in that order — although this naïve numbering system over-represents changes in  $W$  and under-represents changes in  $U$ .

There are a number of observations to be made on Figures 7 and 8. Firstly, there is a very clear difference between the normal plane wave propagation (subplots (a) — (e)) and the abnormal re-entrant behaviour

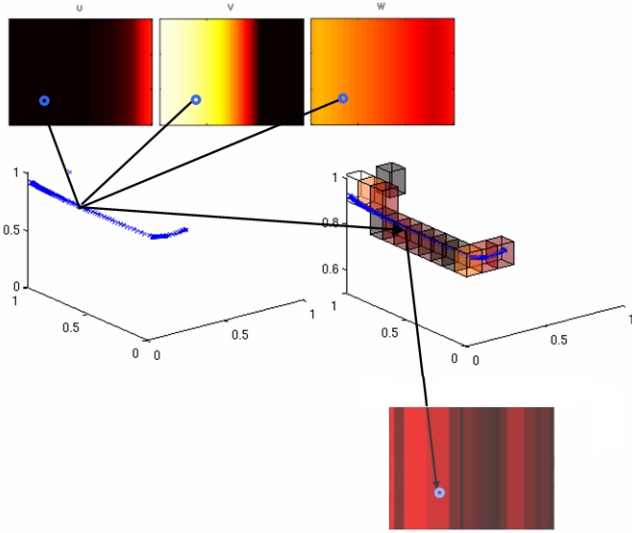


**Figure 6. Forming a ‘hyper-histogram’ image from normal wave propagation through a 2D medium, modelled with Fenton-Karma 3 variable. In this case the cuboids are false coloured by the point counts.**

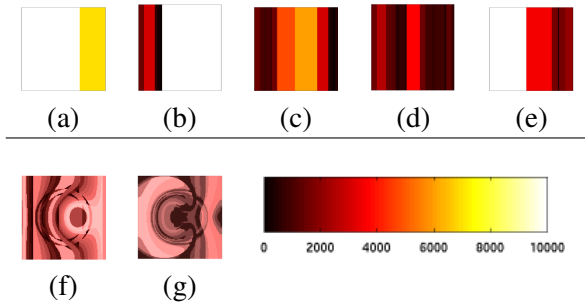


**Figure 7. Visualization of Fenton-Karma 3 Variable model based on ‘hyper-histogram’ counts. (a) – (e) correspond to Figure 4(a) – (e), and (f) and (g) correspond to Figure 5(a) and (b).**

(subplots (f) and (g)). Whereas normal propagation shows a clear ‘banding’ structure, the subplots of re-entrant behaviour are chaotic. Secondly, the underlying heterogeneity that causes the re-entrant behaviour is very clearly visible in subplots (f) and (g), as a double concentric ring structure in the centre of the im-

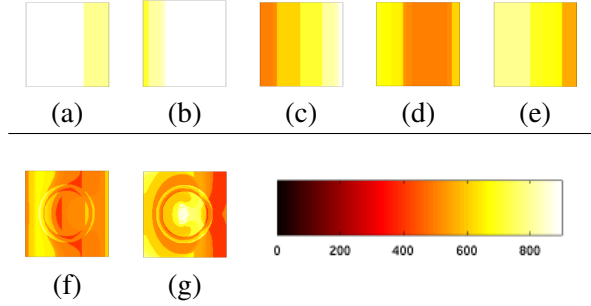


**Figure 8. Visualization of Fenton-Karma 3 Variable model based on ‘hyper-histogram’ ID numbers. (a) – (e) correspond to Figure 4(a) – (e), and (f) and (g) correspond to Figure 5(a) and (b).**

ages. This heterogeneity is only visible directly in images formed from the state variable  $W$ , and not in the images formed from action potential, so it is worth noting it is visible in the combined images. Figure 7 also shows that regions of CVT whose state occupy dense areas of phase-space (shown with light colours) tend to be adjacent to those whose state occupy sparse regions of phase-space (shown with dark colours).

The final observation from Figures 7 and 8 is that they have a significant shortcoming, in that it is very difficult to interpret them physiologically. For instance, it is not possible to tell where the wavefronts of activation are, or similarly at what stage of activation or recovery any given region of CVT is.

## 5 Conclusions and Future Work

In this paper we have presented a novel visualization technique of Cardiac Virtual Tissue based on a hyper-histogram of phase space.

The phase space ‘snake’, and subsequent collapse thereof, itself provides a novel and interesting view of the model, and hopefully could provide some insight into the mechanisms behind the initiation and sustaining of re-entrant behaviour. For instance, is there a cusp at which the collapse of the ‘snake’ becomes inevitable? An extension such as colouring each point in phase space according to its original spatial position may provide further insight, and initial feedback from biologists has been positive.

While the ‘hyper-histogram’ techniques do generate interesting images from an aesthetic point of view, they would also appear to turn a collection of images that can be intuitively understood into a image that can not. On the other hand, the resulting images do seem to combine some of the structural ‘feel’ of the data — such as the underlying heterogeneity — even if these can only be interpreted by comparison with the original multi-image plots. The naïve ‘hyper-histogram’ approach could almost certainly be improved with other clustering metrics, but perhaps a more promising approach would be to move to a model-based visualization. In this case, an empirical model would be built that represents a normal propagation, and then it would be possible to calculate how far from the model any given cell had deviated, and we are currently investigating this.

In the course of this investigation, it became clear that an interactive user interface is essential, with users able to navigate in model time and space. We would also expect techniques such as ‘snap together’ [16] to prove useful.

Although the work presented here has only been applied to CVT, it is interesting to speculate on whether an approach like this could be used to assess the coherence, or lack of coherence, between a collection of movies.

## Acknowledgements

The authors wish to acknowledge the support provided by the funders of the UK e-Science Integrative Biology Project: The EPSRC (ref no: GR/S72023/01) and IBM.

## References

- [1] A. Panfilov and A. Pertsov. Ventricular fibrillation: Evolution of the multiple-wavelet hypothesis. *Philos. Trans. R. Soc. Lond. Ser. A-Math. Phys. Eng. Sci.*, 359:1315–1325, 2001.
- [2] R. Clayton and A. Holden. Filament behaviour in a computational model of ventricular fibrillation in the canine heart. *IEEE Trans. Biomed Eng.*, 51:28–34, 2004.
- [3] F. Xie, Z. Qu, J. Yang, A. Baher, J. N. Weiss, and A. Garfinkel. A simulation study of the effects of cardiac anatomy in ventricular fibrillation. *Journal of Clinical Investigation*, 113:686–693, 2004.
- [4] C. E. Conrath, R. Wilders, R. Coronel, J. M. de Bakker, P. Taggart, J. R. de Groot, and T. Opthof. Intercellular coupling through gap junctions masks M cells in the human heart. *Cardiovascular Research*, 62:407–414, 2004.
- [5] B. Rodríguez, B. M. Tice, J. C. Eason, F. Aguel, J. Jos M. Ferrero, and N. Trayanova. Effect of acute global ischemia on the upper limit of vulnerability: a simulation study. *Am. J. Physiol. Heart. Circ. Physiol.*, 286(6):H2078–H2088, 2004.
- [6] R. Clayton. Computational models of normal and abnormal action potential propagation in cardiac tissue: Linking experimental and clinical cardiology. *Phys. Meas.*, 22:R15–R34, 2001.
- [7] D. Noble and Y. Rudy. Models of cardiac ventricular action potentials: Iterative interactions between experiment and simulation. *Philos. Trans. R. Soc. Lond. Ser. A-Math. Phys. Eng. Sci.*, 359:1127–1142, 2001.
- [8] F. Fenton, E. Cherry, H. Hastings, and S. Evans. Multiple mechanisms of spiral wave breakup in a model of cardiac electrical activity. *Chaos*, 12:852–892, 2002.
- [9] R. Clayton and A. Holden. Propagation of normal beats and re-entry in a computational model of ventricular cardiac tissue with regional differences in action potential shape and duration. *Progress in Biophysics and Molecular Biology*, 85:473–499, 2004.
- [10] D. Simons and C. Chabris. Gorillas in our midst: Sustained inattentive blindness for dynamic events. *Perception*, 28:1059–1074, 1999.
- [11] R. Rensink. When good observers go bad: Change blindness, inattentive blindness, and visual experience. *Psyche*, 6, 2000.
- [12] W. Horrey and C. Wickens. Driving and side task performance: The effects of display clutter, separation, and modality. *Human Factors*, 46(4):611–624, 2004.
- [13] V. Schons and C. Wickens. Visual separation and information access in aircraft display layout. Technical report, University of Illinois, Aviation Research Laboratory, 1993.
- [14] P. Wong and R.D. Bergeron. 30 years of multidimensional multivariate visualization. In G. M. Nielson, H. Hagan, and H. Muller, editors, *Scientific Visualization - Overviews, Methodologies and Techniques.*, pages 3–33, Los Alamitos, CA., 1997. IEEE Computer Society Press.
- [15] R. Gray, A. Pertsov, and J. Jalife. Spatial and temporal organization during cardiac fibrillation. *Nature*, 398:675–678, 1998.
- [16] C. North and B. Shneiderman. Snap-together visualization: Coordinating multiple views to explore information. Technical report, University of Maryland Computer Science Dept., 1999. Technical Report CS-TR-3854.